Theory of the degenerate two-photon laser

A. W. Boone and S. Swain
Department of Applied Mathematics and Theoretical Physics, The Queen's University of Belfast, Belfast BT7 1NN, Northern Ireland
(Received 1 June 1989)

We derive the equation of motion for the field density matrix of the degenerate two-photon laser under conditions of two-photon resonance starting from the full microscopic Hamiltonian. Our results are compared with the corresponding quantities obtained from the standard effective Hamiltonian. As we have shown for the nondegenerate case, the full *diagonal* density-matrix equations tend to the effective Hamiltonian density-matrix equations in an appropriate limit, but the equations of motion for the *off-diagonal* elements do not coincide. The equations obtained using a more accurate form of the effective Hamiltonian, in which Stark shifts are included, do agree. In this paper we concentrate on the photon-number distribution and the nature of the phase transition that takes place in the neighborhood of the two-photon lasing transition threshold. We determine the steady-state mean photon numbers and consider the stability of the solutions. A solution is found where the mean photon number is zero, but this is found to be a stable solution only for sufficiently weak pumping, whereas in the standard effective Hamiltonian approach it is always stable. As the pumping strength is increased, a range of detunings is reached in which there are two stable solutions. The amplitude of the zero-photon peak diminishes very rapidly as the pumping strength increases. Finally, for sufficiently large detunings, a single, stable, steady-state solution is obtained. The nature of the phase transition is illustrated by presenting plots of the photon-number distribution against detuning and pumping rate. The photon-number fluctuations about the mean are also discussed.

I. INTRODUCTION

Although the experimental realization of the two-photon laser as a conventional laser has proved difficult,[1] interest in this system has been rekindled in the last few years by its experimental demonstration as a micromaser[2] and the theoretical prediction of strong correlation between the two modes with its potential for noise reduction.[3] With coherent pumping, it has been shown to exhibit strong squeezing.[4] Most previous theoretical treatments have assumed an *effective* Hamiltonian approach, although the microlaser theory papers[2] and Refs. 5 and 6 are exceptions. The latter treated both the nondegenerate and degenerate cases using the full microscopic Hamiltonian and pointed out the differences in the photon-number distribution for this model as compared with the effective Hamiltonian approach. In a recent publication,[7] where a fuller list of publications on the two-photon laser may be found, we have also considered the difference between the predictions of the effective and full microscopic Hamiltonians for the nondegenerate laser with a three-level atomic scheme. We showed that the equations of motion for the *diagonal* elements of the field density matrix obtained using both approaches coincided in the region where the laser was operating well above threshold and the intermediate level was well off resonance (although they did not coincide otherwise). However, the equations for the *off-diagonal* elements were always found to be distinct. The reason for the failure of the standard effective Hamiltonian approach was traced to the neglect of the Stark shifts induced in the two extreme levels due to the presence of the intermediate state. If the effective Hamiltonian is modified to take account of these shifts, it is found to give an adequate description of the two-photon laser under conditions where the two-photon process dominates the stepwise process. In Ref. 2, a dressed-atom approach has been used which can be shown to be equivalent to a treatment based on the Stark-shifted effective Hamiltonian model. The importance of Stark shifts of the *intermediate* state in the nondegenerate case has been stressed in Ref. 6.

The off-diagonal elements determine such quantities as the linewidths and cross-correlation coefficient. We pointed out that the standard effective Hamiltonian approach gives quite incorrect results for these quantities.

In this paper, we examine the degenerate case and find similar results regarding the validity of the effective Hamiltonian approach. We obtain new expressions for the linewidth and operating frequency shift of the degenerate two-photon laser. However, our principal concern here is with comparing the nature of the steady-state solutions for the mean photon number and their stability. Again, the two approaches give quite different results. The nature of the phase transition is illustrated by plotting the photon-number distributions, and also the mean and variance of the photon number. The plots of the mean photon number show that the two-photon laser could act as a switching device: a small increase in the pumping rate causing a switch from a low mean number state to a high mean number state.

We calculate the density-matrix equation of motion for the field starting from the full microscopic Hamiltonian for a three-level system. This describes more general sit-

uations than the effective Hamiltonian model because it includes both *stepwise* or *cascade* processes and *two-photon* processes. (For an explanation of these terms, see, for example, Ref. 8.) The effective Hamiltonian approach only describes two-photon processes. We calculate the mean photon numbers and examine their stability. In general, the effective Hamiltonian approach leads to different results. Of course, one would not expect it to be a good approximation in situations where the stepwise process is important.

The paper is organized as follows. In Sec. II we obtain the equations of motion for the field density matrix starting from both the microscopic and effective Hamiltonians. Equations for the mean number of photons in each mode are derived in Sec. III. These lead to multiple solutions, and the stability of each solution is investigated: the stability is found to depend upon whether the full or effective Hamiltonian is used. In Sec. IV we compare the expressions for the laser linewidth and frequency shift, and in Sec. V we examine the nature of the phase transition in this system. We present a number of plots of the photon-number distribution, and also show that the equations of motion for the diagonal elements obtained from the full and effective Hamiltonians agree in an appropriate limit. Section VI presents a brief conclusion and summary.

II. EQUATIONS OF MOTION

The basic system for the two-photon laser is shown in Fig. 1. We have a three-level atomic system, with levels $|0\rangle$, $|1\rangle$, and $|2\rangle$ and corresponding energies $\hbar E_0$, $\hbar E_1$, and $\hbar E_2$. A photon of frequency ω connects the $|0\rangle \leftrightarrow |1\rangle$ and $|1\rangle \leftrightarrow |2\rangle$ transitions. The frequency is detuned from the atomic resonances by the detunings

$$\delta_1 \equiv E_{1,0} - \omega, \quad \delta_2 = E_{2,1} - \omega \ . \tag{1}$$

For simplicity, we assume two-photon resonance $\delta_1 = -\delta_2 = -\delta$ throughout this paper.

We adopt the full microscopic Hamiltonian for the degenerate two-photon laser:

$$H = \hbar \left[\sum_{i=0}^{2} |i\rangle\langle i| E_i + a^\dagger a \omega + [(g_1 |1\rangle\langle 0| + g_2 |2\rangle\langle 1|) a + \text{H.c.}] \right] , \tag{2}$$

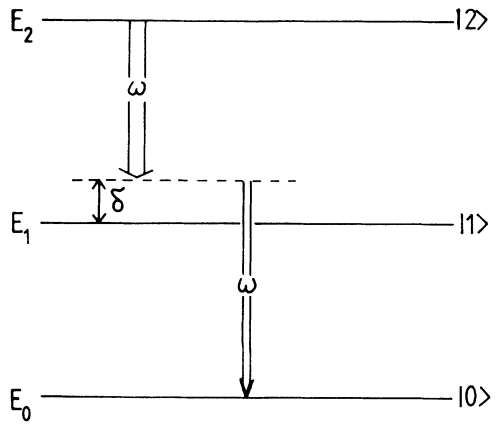

FIG. 1. Atomic level configuration for the degenerate two-photon laser.

where $a^\dagger$ is the creation operator for a photon in the lasing mode and g_1 and g_2 are the usual atom-field coupling constants. The corresponding *effective* Hamiltonian is

$$H_e = \hbar [|0\rangle\langle 0| E_0 + |2\rangle\langle 2| E_2 + a^\dagger a \omega + (g_e |2\rangle\langle 0| a^2 + \text{H.c.})] \ . \tag{3}$$

We have discussed the relationship between these two Hamiltonians in Ref. 7. Here we merely remind the reader that the full Hamiltonian permits both stepwise and direct two-photon transitions whereas in the effective Hamiltonian approach, the atomic level $|1\rangle$ no longer appears explicitly (it plays the role of an intermediate state which is subsumed into the effective Hamiltonian coupling constant $g_e = g_1 g_2 / \delta$) and the basic process is now a direct *two-photon transition* between levels $|0\rangle$ and $|2\rangle$.

Since we have presented in Ref. 7 an outline derivation of the equation of motion of the density matrix for the field in the case of the nondegenerate two-photon laser, and the procedure is the same for the degenerate case, we present just the result here.

Introducing the notation $m = n + k$ and $\rho_{n,m}(t) \equiv \rho_n(k,t)$, we find the following equation of motion for the field density matrix

$$\begin{aligned} \dot{\rho}_n = & -\frac{A_2 \rho_n}{8 d_{n+1}} \Big[8(n+1+k/2) + (n+1)[\sigma_1(n+2+k) + \sigma_2(n+1+k)] \\ & + (n+1+k)[\sigma_1(n+2) + \sigma_2(n+1)] + 4i\bar{\delta} A_2 k - \frac{\sigma_2(n+1)(n+1+k)}{D_{n+1}} F_{n+1} \Big] \\ & + \frac{A_2 [n(n+k)]^{1/2}}{D_n} \rho_{n-1} + \frac{A_2 \sigma_1 [n(n-1)(n+k)(n-1+k)]^{1/2}}{8 D_{n-1} d_{n-1}} F_{n-1} \rho_{n-2} \\ & + C\sqrt{(n+1)(n+k+1)}\,\rho_{n+1} - C(n+k/2)\rho_n \ , \end{aligned} \tag{4}$$

where $A_j=2R|g_j|^2/\gamma^2$, $\sigma_j=4|g_j|^2/\gamma^2\equiv B_j/A_j$, $\bar{\delta}=\delta/\gamma$ (γ being the spontaneous decay rate of each level, which is assumed the same for simplicity, and R the rate at which atoms in their excited state enter the cavity), C is the cavity decay constant and

$$D_n(k)=1+\bar{\delta}^2+S_n+\Sigma/2+\Sigma^2/16 , \tag{5}$$

$$d_n(k)=(1+i\bar{\delta}+S_n/4)[1-i\bar{\delta}+(S_n+\Sigma)/4] , \tag{6}$$

$$F_n(k)=2\bar{\delta}^2+6+3S_n/2+(3-i\bar{\delta})\Sigma/4+\Sigma^2/16 , \tag{7}$$

with $S_n=\sigma_1(n+1)+\sigma_2 n$ and $\Sigma(k)=(\sigma_1+\sigma_2)k$.

In Eq. (4) we have suppressed the dependence of the variables on k because it has the same value for each term, and the time dependence has not been explicitly shown.

The field density matrix obtained using the *effective* Hamiltonian (3) can be found in a similar way. The result is much simpler:

$$\dot{\rho}^e_n(k)=\frac{\rho^e_n}{D^e_{n+1}}[A^e(n+1)(n+2)+A^eK_{n+1}(1-i\Delta)/2+B^eK^2_{n+1}/8] + \frac{A^e[n(n-1)(n+k)(n-1+k)]^{1/2}}{D^e_{n-1}}\rho^e_{n-2}+C\sqrt{(n+1)(n+k+1)}\rho^e_{n+1}-C(n+k/2)\rho^e_n , \tag{8}$$

where Δ is the detuning of the two-photon transition from exact resonance

$$\Delta=(E_2-E_0-\omega_1-\omega_2)/\gamma , \tag{9}$$

$$D^e_n=1+\Delta^2+\sigma_e[n(n+1)+K_n/2]+(\sigma_eK_n/4)^2 , \tag{10}$$

$$K_n=(2n+1)k+k^2 , \tag{11}$$

and the quantities A^e, B^e, and σ_e are as defined below Eq. (4) with g_1 and g_2 both replaced by g_e. In the derivation of Eq. (4) we assumed two-photon resonance, and so to compare Eqs. (4) and (8) we should set $\Delta=0$. (Note that the effective Hamiltonian strictly applies only for two-photon resonance.)

We note that the above equations for the degenerate case can be obtained from those for the nondegenerate case [Eqs. (5)–(13) of Ref. 7] by the following replacements:

$$\omega_1\to\omega_2\to\omega, \quad C_1\to C_2\to C ,$$

$$n_2\to n, \quad n_1\to n+1, \quad k_1\to k_2\to k ,$$

and

$$\rho_{n_1+i,n_2+j}(k_1,k_2)\to\rho^e_{n+i+j}(k) . \tag{12}$$

In the next section we calculate and compare the mean photon numbers for both models.

III. MEAN PHOTON NUMBERS—SEMICLASSICAL THEORY

The microscopic and effective Hamiltonian models lead to different estimates in general for the mean photon number in the steady state. This quantity is calculated by setting

$$\dot{\bar{n}}=\sum_n n\rho_n(0)=0 , \tag{13}$$

using Eqs. (4) and (8). For the microscopic model we find

$$\dot{\bar{n}}=\sum_n\rho_n(0)\left[\frac{3A_2\sigma_1(n+1)(n+2)(1+S/4+\bar{\delta}^2/3)}{2(1+\bar{\delta}^2+S)(1+\bar{\delta}^2+S/2+S^2/16)} + \frac{A_2(n+1)}{1+\bar{\delta}^2+S}-Cn\right]=0 , \tag{14}$$

where $S\equiv S_{n+1}(0)$ and $\rho_n(0)$ denotes the diagonal elements in the steady state. Next we assume that $\rho_n(0)$ is a sharply peaked function of n centered on $n=\bar{n}$. (Later we calculate the value of $\rho_n(0)$ numerically, so that the validity of this assumption may be assessed.) We may then replace n inside the parentheses by $\bar{n}$ to obtain

$$\frac{3A_2\sigma_1(\bar{n}+1)(\bar{n}+2)(1+\bar{S}/4+\bar{\delta}^2/3)}{2(1+\bar{\delta}^2+\bar{S})(1+\bar{\delta}^2+\bar{S}/2+\bar{S}^2/16)}+\frac{A_2(\bar{n}+1)}{1+\bar{\delta}^2+\bar{S}} =C\bar{n} , \tag{15}$$

where $\bar{S}\equiv S_{\bar{n}+1}(0)$.

Next we restrict the theory to the semiclassical case by neglecting the spontaneous-emission contributions in Eq. (15). This is valid when $\bar{n}\gg 1$, so that we can replace $n+1$ and $\bar{n}+2$ in the above equation by $\bar{n}$. It is clear that in the semiclassical theory, $\bar{n}=0$ is always a steady state. The remaining factors give a cubic equation for $\bar{n}$ which may be written in the form

$$(4z+\bar{\delta}^2-3)(z^2+\bar{\delta}^2) =\mu[z^2+\bar{\delta}^2+\tfrac{3}{2}\sigma_1\bar{n}(z+\bar{\delta}^2/3)] , \tag{16}$$

where

$$\mu=A_2/C, \quad z=1+(\sigma_1+\sigma_2)\bar{n}/4 . \tag{17}$$

This is exactly equivalent to the equation obtained by Zhu and Li [Ref. 5, Eq. (42)]. These authors, however, used the condition $\rho_n(0)=\rho_{n+1}(0)$ as the definition of $\bar{n}$. For a laser operating well above threshold, the approxi-

mation $\bar{n} \gg 1$ is excellent.

The cubic has a simple solution when

$$\sigma_1 = \sigma_2 \equiv \sigma \ . \tag{18}$$

Then we find the unphysical root $\sigma\bar{n} = -(\bar{\delta}^2+1)/2$ and the pair of roots $\sigma\bar{n} = \mu - 2 \pm (\mu^2 - 4\bar{\delta}^2)^{1/2}$. The latter solutions are physical only for $\mu \geq 2|\delta|$.

A linear stability analysis indicates that the $\bar{n}=0$ solution is stable only if $\mu < 1+\bar{\delta}^2$ and that the solution with the negative square root is always unstable. The solution with the positive square root is found to be stable if $\mu \geq 1+\bar{\delta}^2$ for $\bar{\delta}^2 \leq 1$ and for $\mu \geq 2|\bar{\delta}|$ for $\bar{\delta}^2 \geq 1$. The two stable solutions are thus

$$\bar{n}^{(1)} = 0, \quad \sigma\bar{n}^{(2)} = \mu - 2 + (\mu^2 - 4\bar{\delta}^2)^{1/2} \ . \tag{19}$$

Hence for a fixed value of $\bar{\delta}^2 \leq 1$, there is only one stable solution for a given value of μ: the solution $\bar{n}^{(1)}=0$ is stable for $\mu \leq 1+\bar{\delta}^2$ and the solution $\bar{n}^{(2)}$ is stable for $\mu \geq 1+\bar{\delta}^2$. In particular, for $\delta=0$, $\bar{n}^{(1)}=0$ is the stable solution for $\mu<1$ and $\sigma\bar{n}^{(2)}=2(\mu-1)$ is the stable solution for $\mu>1$.

On the other hand, *both* solutions are stable for $\bar{\delta}^2 > 1$ and

$$2 < 2|\delta| \leq \mu < 1+\bar{\delta}^2 \ . \tag{20}$$

Later we plot the photon-number distribution, showing the presence of two peaks under these conditions.

For the effective Hamiltonian, we find the solutions

$$\bar{n}_e^{(1)} = 0, \quad \sigma_e \bar{n}_e^{(2)} = \mu_e \pm [\mu_e^2 - \sigma_e(1+\Delta^2)]^{1/2} \ , \tag{21}$$

where $\mu_e \equiv A^e/C$. We find that the $\bar{n}_e^{(1)}=0$ solution is always stable, that the negative branch of the $\bar{n}_e^{(2)}$ solution is always unstable, and that the positive branch is stable for $\mu_e \geq [\sigma_e(1+\Delta^2)]^{1/2}$, which is the condition for the solutions to be real.

Taking $\Delta=0$ for comparison with the microscopic results, we then have a single stable solution $\bar{n}_e=0$ for pumping strengths such that $\mu_e < \sqrt{\sigma_e}$ and two stable solutions, $\bar{n}_e^{(1)}=0$, and $\sigma_e\bar{n}_e^{(2)} = \mu_e + (\mu_e^2 - \sigma_e)^{1/2}$ for $\mu_e > \sqrt{\sigma_e}$.

These results on the stability of solutions are quite different from those for the microscopic Hamiltonian. In particular, for the latter case, the solution at the origin is unstable for $1+\bar{\delta}^2 < \mu$. The source of this behavior is that, as the intermediate-state detuning approaches zero, the system tends to the one-photon laser limit (cascade process) where the gain is linear in n, thus rendering the zero-photon solution unstable above threshold.

As in the case of the nondegenerate laser, the equations of motion for the diagonal field density-matrix elements obtained using the microscopic Hamiltonian coincide approximately with those obtained from the effective Hamiltonian provided that the conditions

$$\gamma|\delta| \ll |g|^2\bar{n} \ll \delta^2, \quad \sigma_1 \simeq \sigma_2 \tag{22}$$

are satisfied. This is shown in Sec. V. We have used the fact that $\sigma_1 \simeq \sigma_2$ implies $|g_1| \simeq |g_2| \equiv |g|$. The first part of the inequality is the condition for the laser to be operating far above threshold while the second part is the condition that the power broadening (or, equivalently, the Rabi splitting) of the intermediate state be much less than the detuning. This is just the condition for the laser to be operating as a two-photon, rather than a stepwise, system.

The analysis leads to the correspondences

$$A^e = \frac{A_2\sigma_1}{4\bar{\delta}^2}, \quad \sigma_e = \frac{\sigma_1\sigma_2}{4\bar{\delta}^2} \ . \tag{23}$$

The latter expression is consistent with the relation $|g_e| = |g_1 g_2/\delta|$, which is implied by the perturbative construction of the effective Hamiltonian. Using Eqs. (23), it is easy to show that Eq. (21) reduces to Eq. (19) under conditions (22) (and with $\sigma_1=\sigma_2$).

However, the *off-diagonal* equations of motion do not coincide, even under the conditions (22). This is demonstrated indirectly in the next section where we calculate quantities that are determined by the off-diagonal elements. As we have shown in Ref. 7, the reason for this failure of the effective Hamiltonian approach can be traced to the neglect of Stark shifts. In the three-level model, the interaction of the two extreme levels with the intermediate state $|1\rangle$ via the electromagnetic field causes a shift of their energies from the bare values E_0 and E_2 as given in Eq. (3). If these shifts are correctly incorporated, the resulting effective Hamiltonian provides a satisfactory model for the two-photon laser operating under the conditions (22).

IV. LINEWIDTHS AND CROSS-CORRELATION COEFFICIENT

These quantities are calculated as in Ref. 3 by evaluating the time derivative of the quantity

$$y(t) \equiv \sum_n \rho_n(k) \ , \tag{24}$$

using Eq. (4). By manipulating the sums on the right-hand side it may be written in the form

$$\dot{y} = -\nu(k) y \ , \tag{25}$$

where

$$\nu(k) = \frac{iA_2\bar{\delta}k}{2N}\left[1 - \frac{(\sigma_1+\sigma_2)k}{2N}\right] + \frac{k^2}{8\bar{n}}\left[\frac{A_2(1+S)}{N} + C\right] , \tag{26}$$

with

$$N = 1+\bar{\delta}^2+S, \quad S = (\sigma_1+\sigma_2)\bar{n} \ . \tag{27}$$

The imaginary part of $\nu(1)$ represents a frequency shift; that is, the operating frequency of the laser is shifted from the cavity frequency ω to the new operating frequency Ω

$$\Omega = \omega + \mathrm{Im}[\nu(1)] = \omega + \frac{A_2\bar{\delta}}{2N}\left[1 - \frac{(\sigma_1+\sigma_2)}{2N}\right] . \tag{28}$$

The *real part* $\mathrm{Re}[\nu(1)]$ is equal to the *linewidth* of the laser mode. Thus the linewidth is

$$b=\frac{1}{8\bar{n}}\left[\frac{A_2(1+S)}{N}+C\right] . \tag{29}$$

When $\bar{\delta}=0$, $N=1+S$ and thus the above expression reduces to

$$b=\frac{A_2+C}{8\bar{n}} . \tag{30}$$

The same result is a good approximation for $\delta\neq 0$ when the laser is operating well above threshold so that $S\gg 1+\bar{\delta}^2$. Equation (30) is formally identical to the single-mode laser result, but we must remember that the definition of $\bar{n}$ is different. For example, for $\delta=0$ or $\mu\gg 2|\bar{\delta}|$ we have $\sigma\bar{n}^{(2)}=2(\mu-1)$ from Eq. (19), or

$$\bar{n}^{(2)}=2(A-C)/\sigma , \tag{31}$$

where $\sigma=B_1/A_1=B_2/A_2$. This is just twice the single-mode result $\bar{n}_{\mathrm{SM}}=A(A-C)/BC$.

For the effective Hamiltonian the same procedure yields the results

$$\nu_e(k)=-i\frac{A^e k\Delta}{2N_e}\left[2\bar{n}_e+\frac{(k+3)(1+\Delta^2-\sigma_e n_e^2)}{N_e}\right]$$
$$+k^2\left[\frac{A^e}{2N_e}(1+\sigma_e\bar{n}_e^{\,2})+\frac{C}{8\bar{n}}\right] , \tag{32}$$

where $N_e=1+\Delta^2+\sigma_e\bar{n}_e^{\,2}$ (for $\bar{n}_e\gg 1$). The laser linewidth is given by the real part of the coefficient of k^2. The imaginary term yields the frequency shift.

$$\Omega_e=\omega_e-\frac{\Delta A^e\bar{n}_e}{1+\Delta^2+\sigma_e^2\bar{n}_e^{\,2}} , \tag{33}$$

which is the approximately the expression obtained by Wang and Haken[9] in their investigations using the effective Hamiltonian approach. In the limit $\Delta=0$, or $\sigma_e\bar{n}^{\,2}\gg 1+\Delta^2$, the imaginary term vanishes (no frequency shifts) and the laser linewidth is given by

$$b_e=\frac{A^e}{2}+\frac{C}{8\bar{n}_e} . \tag{34}$$

Well above threshold, the first term on the right-hand side dominates the second, and the result for the linewidth in the effective Hamiltonian approximation is clearly quite different from that for the linewidth obtained from the microscopic Hamiltonian. Under conditions (22), and for $\sigma_1=\sigma_2$, Eq. (29) reduces to $b=A^e+C/8\bar{n}_e$, using the correspondences (23). Hence, well above resonance, the effective Hamiltonian approach gives a value for the linewidth which is one-half that obtained using the full theory.

V. PHOTON-NUMBER DISTRIBUTION

In this section we evaluate the probability $p(n)$ that the field contains n photons for the steady state: $p(n)\equiv\rho_n(0)$, by solving numerically the difference equation that results from setting $\dot{\rho}(0)=0$ in Eq. (4). The solution is facilitated by the observation of Zhu and Li[5] that the resulting five-term difference equation may be expressed as the difference of two three-term difference equations of the form

$$C(n+1)p(n+1)=[\alpha(n)+\beta(n)]p(n)$$
$$+\beta(n-1)p(n-1) , \tag{35}$$

where

$$\alpha(n)=\frac{A_2(n+1)}{1+\bar{\delta}^2+S_{n+1}} \tag{36}$$

and

$$\beta(n)=\frac{3A_2\sigma_1(n+1)(n+2)(1+\bar{\delta}^2/3+S_{n+1}/4)}{4(1+\bar{\delta}^2+S_{n+1})(1+\bar{\delta}^2+S_{n+1}/2+S_{n+1}^2/16)} . \tag{37}$$

From the effective Hamiltonian approach, we may derive the three term recurrence relation

$$C(n+1)p_e(n+1)=\beta_n^e p_e(n)+\beta_{n-1}^e p_e(n-1) , \tag{38}$$

where

$$\beta_n=\frac{A^e(n+1)(n+2)}{D+\sigma_e(n+1)(n+2)} . \tag{39}$$

It is easy to see from Eqs. (35)–(39) in the case where $\sigma_1\simeq\sigma_2$ that $p(n)\rightarrow p_e(n)$ for $n\gg 1$ when the conditions (22) apply. The latter imply $\gamma|\delta|\ll S_n\ll\delta^2$, and imposing these conditions on Eqs. (36) and (37) we see that $\alpha(n)\ll\beta(n)$ and that

$$\beta(n)\rightarrow\frac{A_2\sigma_1(n+1)(n+2)}{4\bar{\delta}^2(1+S_{n+1}^2/16\bar{\delta}^2)} . \tag{40}$$

For $\sigma_1\simeq\sigma_2$ and $n\gg 1$, we have $S_{n+1}^2\simeq 4\sigma_1\sigma_2(n+1)(n+2)$ and then using the equivalences (23) we see that the right-hand sides of Eqs. (35) and (38) are equal (for $\Delta=0$).

We have evaluated expressions (35) and (38) numerically. The graphs show quite sharp features, and to show these up more clearly, we have chosen smaller values for the parameters σ_1, σ_2, and $\bar{\delta}$ than are likely to occur in actual two-photon lasers. In Figs. 2–8 we have taken $\sigma_1=\sigma_2=4\times 10^{-2}$. For Fig. 2 we have $\bar{\delta}=0$. This distribution shows no bistable behavior: the solution $\bar{n}^{(1)}=0$ is stable for $\mu<1$ and the solution $\bar{n}^{(2)}=50(\mu-1)$ is stable for $\mu\geq 1$. [We are assuming that the positions of the peaks of the distribution are given approximately by Eqs. (19).] In Fig. 3 we have the same parameters except that $\bar{\delta}=1$. This again shows no bistable behavior, with $\bar{n}^{(1)}=0$ being stable for $\mu<2$ and $\bar{n}^{(2)}=50(\mu-2)$ being stable for $\mu\geq 2$. Figures 2 and 3 are qualitatively similar with a smooth transition from the peak at $\bar{n}_1$ to the peak at $\bar{n}_2$ as μ increases.

We note that the quoted values for $\bar{n}$ were derived on the assumption that $p(n)$ was a sharply peaked function of n centered on $n=\bar{n}^{(2)}\gg 1$. This assumption is clearly not justified for the case of Figs. 2 and 3, where the peaks

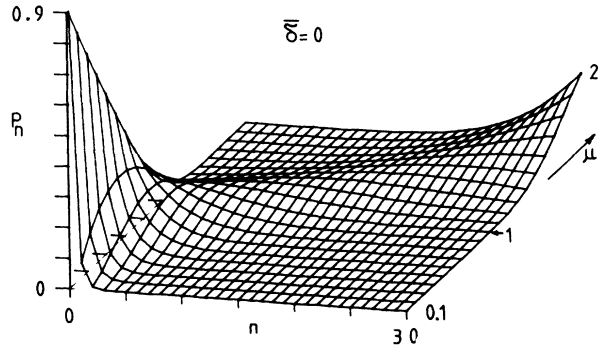

FIG. 2. Photon-number distribution as a function of the pumping rate $\mu = A/C$ for $\sigma_1 = \sigma_2 = 0.04$ and $\bar{\delta} = 0$.

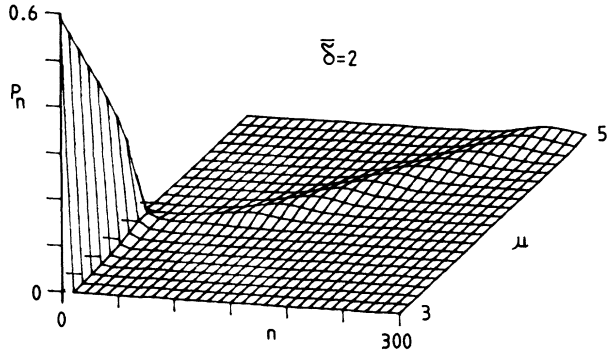

FIG. 4. As Fig. 1, but with $\bar{\delta} = 2$.

are very flat in the neighborhoods of the critical values of μ, but nevertheless Eq. (19) gives the approximate position of the peaks of the distribution reasonably well. As we have previously observed, Zhu and Li[5] obtained the same equation [Eq. (15)] by finding the values of n for which $p(n) = p(n \pm 1)$. This perhaps explains why the fit is better than expected on the basis of our assumptions.

In Fig. 4, where the value of $\bar{\delta}$ has been increased to 2, we begin to see a qualitative change. Now we have bistable behavior over the range $4 < \mu < 5$, although this is not evident from the figure. The switch over from the peak at $\bar{n}^{(1)} = 0$ to the peak at $\bar{n}^{(2)} = 25[\mu - 2 + (\mu^2 - 16)^{1/2}]$ is becoming sharper. This feature becomes more apparent in Fig. 5, where we have taken $\bar{\delta} = 3$. The bistable behavior extends over the range $6 < \mu < 10$, and the peak at $\bar{n}^{(1)} = 0$ tends to zero very rapidly for $\mu > 6.25$. The peak at $\bar{n}^{(2)} = 25[\mu - 2 + (\mu^2 - 36)^{1/2}]$, and the general features in the critical region $\mu \sim 6$ are not prominent in this figure, so we have displayed this region in more detail in the following two figures. In Fig. 6, the emergence of the second peak is shown around the critical value $\mu = 6$. The high peak at $\bar{n}^{(1)} = 0$ has been excluded so that the second peak can be seen more clearly. In Fig. 7 we have plotted out the region $6.5 < \mu < 6.75$. Note Eq. (19) predicts $\bar{n}^{(2)} = 175$ for $\mu = 6.5$, and one can see from the figure that this is close to the exact value for which $p(n)$ has a maximum, even though $p(n)$ is not very sharply peaked about $n = \bar{n}^{(2)}$. The peak is, however, nearly symmetric about $n = \bar{n}^{(2)}$ so that the criterion of Zhu and Li applies.

In Fig. 5, the persistence of the peak at $\bar{n} = 0$ beyond $\mu \simeq 7$ is not apparent, although Eq. (20) predicts that it should exist out to $\mu = 10$. In Fig. 8, we have plotted on an extended scale the region around $\mu = 10$ for small values of n, and it can indeed be seen that a shallow minimum does exist near $n = 3$ for $\mu = 9.5$, which has disappeared for $\mu \geq 10$.

If we decrease the value of σ_1 and σ_2 (which means increasing the mean value $\bar{n}_2$) then the sharpness of the decline of the peak at $\bar{n}^{(1)} = 0$ near the critical value $\mu = 2|\bar{\delta}|$ is increased. This feature is illustrated in Fig. 9, where we have taken $\sigma_1 = \sigma_2 = 10^{-2}$. This should be compared with Fig. 5. As we have previously observed, increasing the value of δ has a similar effect.

If we plot the density matrix $p_e(n)$ obtained from the effective Hamiltonian by solving Eq. (38) for parameter values corresponding to those of Fig. 5 (i.e., $\sigma_e = \frac{4}{9} \times 10^{-4}$, $\frac{3}{9} \times 10^{-2} < \mu_e < \frac{8}{9} \times 10^{-2}$), we obtain graphs which look quite different from those of Fig. 5. This is because we are operating in a regime where the condition (22) is *not* satisfied. We do not present this plot because it is rather featureless: only the peak at $\bar{n}^{(1)} = 0$ is apparent, and this has uniform height. In Fig. 10, we do give a plot of the effective Hamiltonian results, where we have chosen the parameters to ensure that bistable behavior is displayed. We have taken $\sigma_e = 4 \times 10^{-2}$ and $0.025 < \mu_e < 0.60$. From Eq. (21), two peaks should exist

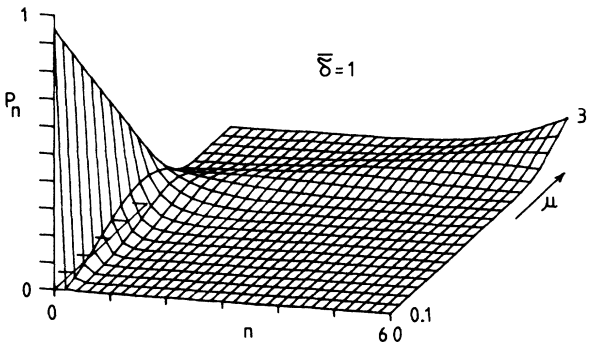

FIG. 3. As Fig. 1, but with $\bar{\delta} = 1$.

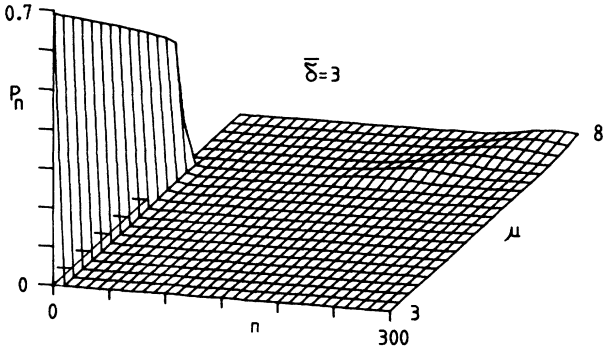

FIG. 5. As Fig. 1, but with $\bar{\delta} = 3$.

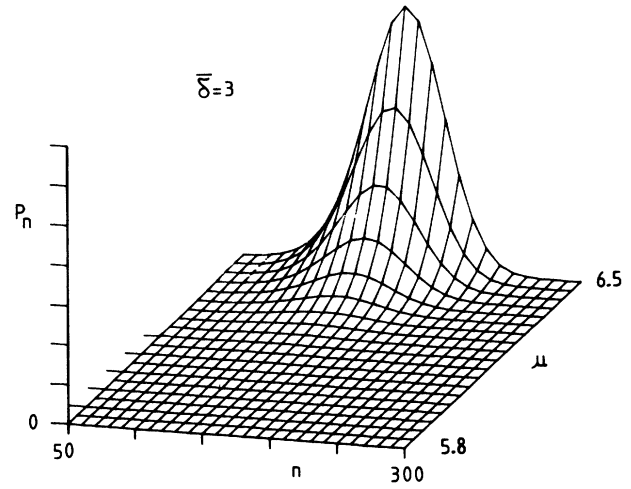

FIG. 6. As Fig. 5, but with $5.8 \leq \mu \leq 6.5$.

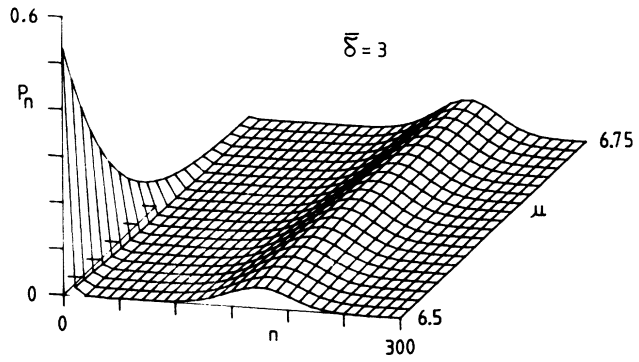

FIG. 7. As Fig. 5, but with $6.5 \leq \mu \leq 6.75$.

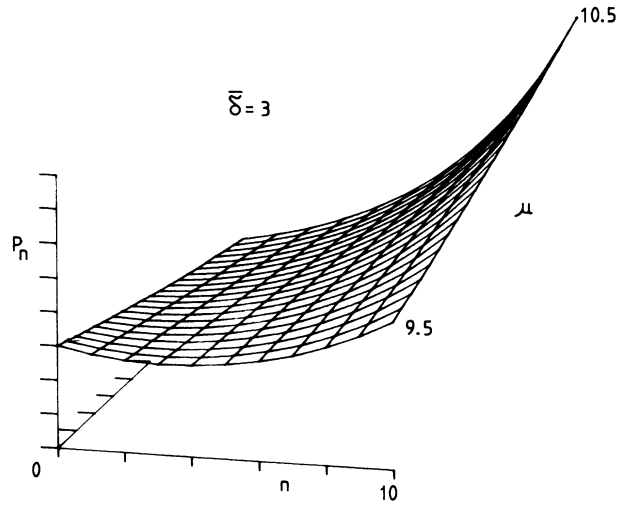

FIG. 8. As Fig. 1, but with $9.5 \leq \mu \leq 10.5$.

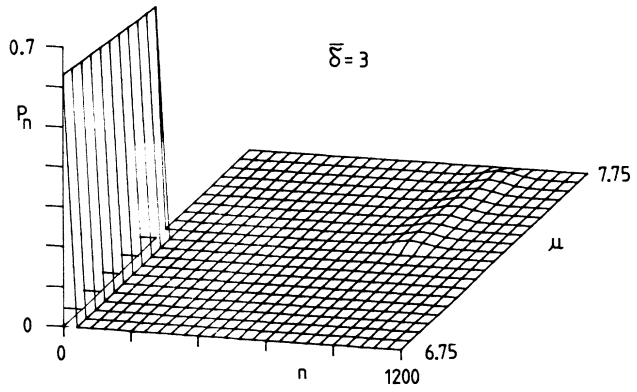

FIG. 9. As Fig. 5, but with $\sigma_1=\sigma_2=0.01$ and $7 \leq \mu \leq 7.025$.

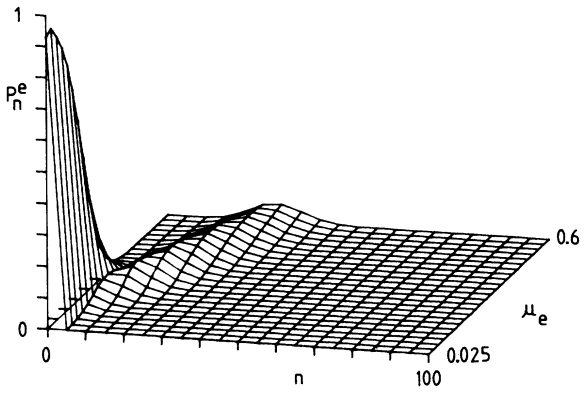

FIG. 10. Photon-number distribution from the effective Hamiltonian approach with $\sigma_1=0.04$.

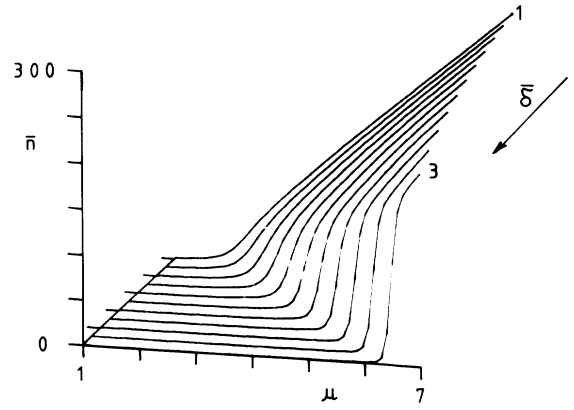

FIG. 11. Mean photon number as a function of $\bar{\delta}$ and μ.

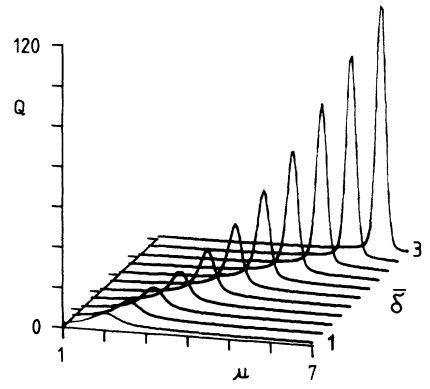

FIG. 12. Variance in the photon-number distribution, as measured by the Q parameter, as a function of $\bar{\delta}$ and μ.

for $\mu_e > 0.2$, but the peak at $\bar{n}^{(1)}=0$ becomes very shallow for $\mu_e > 0.3$ and is not apparent on the figure.

In order to operate where condition (22) applies, we must have $|\bar{\delta}| \geq 100$. Taking $\bar{\delta}=100$, for example, we can satisfy condition (22) by taking $|g|^2\bar{n} \simeq 10^3\gamma^2$ and then the condition gives $10^2\gamma^2 \ll |g|^2\bar{n} \ll 10^4\gamma^2$, which is modestly satisfied. Then, as we have shown analytically, the density matrices obtained using the two approaches agree approximately. We have verified this numerically.

Finally, we look at other properties of the system that are strongly influenced by the phase transition. First we plot the mean photon number [obtained from the numerical solution of Eq. (19)] as a function of $\bar{\delta}$ and μ in Fig. 11. The increasing sharpness of the transition from a low photon-number state to a high photon-number state as $|\bar{\delta}|$ increases is obvious. Again, we have chosen particularly small values for $|\bar{\delta}|$ which diminish the abruptness of the change so that the effects can be more clearly seen. There is thus the possibility of using the two-photon laser as a switching device, as the switch from low to high photon number is accomplished by only a very small increase in the pumping rate. In Fig. 12, as a measure of the spread of photon numbers about the mean, we plot the "Q parameter"

$$Q \equiv [\mathrm{Var}(n) - \bar{n}]/\bar{n} \tag{41}$$

for the same range of parameters as in Fig. 11 (but note the change in the sense of increasing $|\bar{\delta}|$ between Figs. 11 and 12). The latter indicates the increasing intensity and sharpness of the photon-number fluctuations near the critical values of μ as $|\bar{\delta}|$ increases. We note that the fluctuations are always super-Poissonian.

As δ is reduced, these two figures clearly show the change from the "first-order phase-transition" picture, typical of two-photon lasers, to the "second-order phase-transition" regime, characteristic of one-photon oscillators.

VI. CONCLUSION

We have derived the equations of motion satisfied by the field density matrix of the two-photon laser starting from the full microscopic Hamiltonian. Possible solutions for the mean photon numbers in the laser mode in the steady state have been found and their stability investigated. We have also calculated the laser linewidth and the shift in the lasing frequency. These results have been compared with those obtained from the effective Hamiltonian. The effective Hamiltonian only includes two-photon processes, whereas the microscopic Hamiltonian also includes stepwise processes. We have found agreement for the diagonal elements of the field density matrices only under conditions (22), and for $\sigma_1 \simeq \sigma_2$. The equations for the off-diagonal elements do not agree, even under conditions (22). Under these conditions we find that the effective Hamiltonian underestimates the laser linewidth by a factor of 2. This is because the usual form of the effective Hamiltonian models the atom as a two-level system and neglects the Stark shifts induced in these levels by their interaction with the intermediate state(s). If these shifts are properly included, then the resulting effective Hamiltonian model provides an adequate basis for the two-photon laser operating under conditions (22). The importance of the Stark shifts of the outer two levels, obtained in the different approach of the dressed-atom model, has already been pointed out in Ref. 2. These results imply that the linewidth and frequency shift depend strongly on the detailed atomic structure.

The importance of Stark shifts has also been emphasized by Zhu and Scully[6] in a different context. They considered the nondegenerate two-photon laser, not necessarily operating under conditions of two-photon resonance, and showed that the Stark shift of the *intermediate* state could affect the photon distribution by shifting the transition frequencies of the system.

We have investigated the nature of the phase transition in this system both analytically and by numerical solution of the difference equations for the photon-number probabilities. The transition has been shown to be very sharp for small values of σ_1 and σ_2 and large values of $\bar{\delta}$. A switch from small mean photon number to large mean photon number is accomplished by a very small change in the pumping rate. We have presented plots of the mean photon number and Mandel's Q factor that also indicate the nature of the phase transition.

ACKNOWLEDGMENTS

One of us (A.W.B.) wishes to thank the Department of Education for Northern Ireland for financial support.

[1]B. Nikolaus, D. Z. Zhang, and P. E. Toschek, Phys. Rev. Lett. **47**, 171 (1981); G. Grynberg, E. Giacobino, and F. Biraben, Opt. Commun. **36**, 403 (1981); J. Y. Gao, W. W. Eidson, M. Squicciarini, and L. M. Narducci, J. Opt. Soc. Am. B **1**, 606 (1984).

[2]M. Brune, J. M. Raimond, and S. Haroche, Phys. Rev. A **35**, 154 (1987); L. Davidovich, J. M. Raimond, M. Brune, and S. Haroche, *ibid.* **36**, 3771 (1987); M. Brune, J. M. Raimond, P.

Goy, L. Davodovich, and S. Haroche, Phys. Rev. Lett. **59**, 1899 (1987); IEEE J. Quantum Electron. **24**, 1323 (1988).
[3]S. Swain, J. Mod. Opt. **35**, 103 (1988).
[4]M. O. Scully, K. Wodkiewicz, M. S. Zubairy, J. Bergou, Ning Lu, and J. Meyer ter Vehn, Phys. Rev. Lett. **60**, 1382 (1989).
[5]Shi-Yao Zhu and Xiao-Shen Li, Phys. Rev. A **36**, 3889 (1987).
[6]Shi-Yiao Zhu and M. O. Scully, Phys. Rev. A **38**, 5433 (1988).
[7]A. W. Boone and S. Swain, Quantum Opt. **1**, 27 (1989).
[8]D. P. O'Brien and S. Swain, J. Phys. B **16**, 2499 (1983).
[9]Z. C. Wang and H. Haken, Z. Phys. **55**, 361 (1984); **56**, 77 (1984); **56**, 83 (1984).